THE UNIVERSITY OF
WARWICK

University of Warwick institutional repository: http://go.warwick.ac.uk/wrap

This paper is made available online in accordance with
publisher policies. Please scroll down to view the document
itself. Please refer to the repository record for this item and our
policy information available from the repository home page for
further information.

To see the final version of this paper please visit the publisher's website.
Access to the published version may require a subscription.

Author(s): I. Mahboob, T. D. Veal, and C. F. McConville
Article Title: Electron dynamics in InN_xSb_{1-x}

Year of publication: 2003
Link to published version: http://dx.doi.org/10.1063/1.1611270
Publisher statement: None

Electron dynamics in InN_xSb_{1-x}

I. Mahboob, T. D. Veal, and C. F. McConville[a)]
Department of Physics, University of Warwick, Coventry, CV4 7AL United Kingdom

(Received 9 May 2003; accepted 23 July 2003)

Electron transport properties in InN_xSb_{1-x} are investigated for a range of alloy compositions. The band structure of InN_xSb_{1-x} is modeled using a modified **k·p** Hamiltonian. This enables the semiconductor statistics for a given x value to be calculated from the dispersion relation of the E_- subband. These calculations reveal that for alloy compositions in the range $0.001 \leqslant x \leqslant 0.02$ there is only a small variation of the carrier concentration at a given plasma frequency. A similar trend is observed for the effective mass at the Fermi level. Measurements of the plasma frequency and plasmon lifetime for InN_xSb_{1-x} alloys enable the carrier concentration and the effective mass at the Fermi level to be determined and a lower limit for the electron mobility to be estimated. © *2003 American Institute of Physics.* [DOI: 10.1063/1.1611270]

The partial replacement of group V atoms in III–V semiconductors with small, isoelectronic, and highly electronegative nitrogen atoms results in the formation of dilute nitrides; a class of semiconductor alloy with highly unusual electronic properties.[1] Although extensive optical measurements of the large band gap bowing in III–N–Vs have been undertaken, the electronic transport properties of these materials have received little attention.[2] The major factor is the profound change of the conduction band resulting from the incorporation of the nitrogen. Hence, models of electron transport employing an energy independent electron effective mass are no longer applicable.[3] In this letter, we present calculations of the semiconductor statistics for InN_xSb_{1-x} for $0.001 \leqslant x \leqslant 0.02$. Measurements of the plasma frequency and the plasmon lifetimes enable the mobility of the electrons, the carrier concentration, and the effective mass of the carriers at the Fermi level to be determined, thus defining all the transport properties in InN_xSb_{1-x}.

The introduction of nitrogen into a III–V semiconductor results in the formation of a narrow resonant nitrogen band that is situated close to the conduction band edge. The interaction of the extended Γ states of the conduction band of the host semiconductor with the localized N-induced resonant states results in the formation of two nonparabolic subbands E_- and E_+ whose dispersion is modeled using a modified **k·p** Hamiltonian.[4] The E_- band has mainly conduction band-like character, whereas the E_+ subband is due to the E_N-like states. The parameters for the modified **k·p** Hamiltonian have been determined by fitting the resulting $E_\pm$ subbands to the tight binding band structure of InN_xSb_{1-x}. Details of the tight binding calculation can be found in Ref. 4 and references therein. The dispersion of the $E_\pm$ subbands can be determined by finding the eigenvalues of the 2×2 determinant

$$\begin{vmatrix} E_M - E & \beta\sqrt{x} \\ \beta\sqrt{x} & [E_N - (\alpha+\gamma)x] - E \end{vmatrix} = 0, \tag{1}$$

where $\alpha = 2.44$ eV, $\beta = 1.99$ eV, $\gamma = 2.47$ eV, $E_N = 0.74$ eV is the nitrogen level, and E_M is the host conduction band.[5] The change in the nitrogen level due to the increased concentration of N pairs with increasing x content is accounted for by γ in the earlier expression. However, this becomes a 5×5 Hamiltonian when conventional **k·p** theory is included to account for the intrinsic nonparabolicity of the host InSb due to the interaction between the valence bands and the conduction band.

The conduction band profiles for InN_xSb_{1-x} are shown in Fig. 1 for a range of x values calculated from the modified **k·p** Hamiltonian. The conduction bands found in InSb and a hypothetical InSb-like semiconductor with a constant effective mass are plotted for comparison. The parabolic dispersion relation in this figure which arises from a constant effective mass is not a valid description of the conduction band dispersion in InSb as this model ignores the interaction of the conduction band with the valence bands. The intrinsic nonparabolicity found in InSb can be described by a four band Kane model[6] which results in an energy dependent effective mass. The conduction band dispersion in InN_xSb_{1-x} is significantly different from that in InSb. The interaction of the nitrogen level with the conduction band causes the band gap

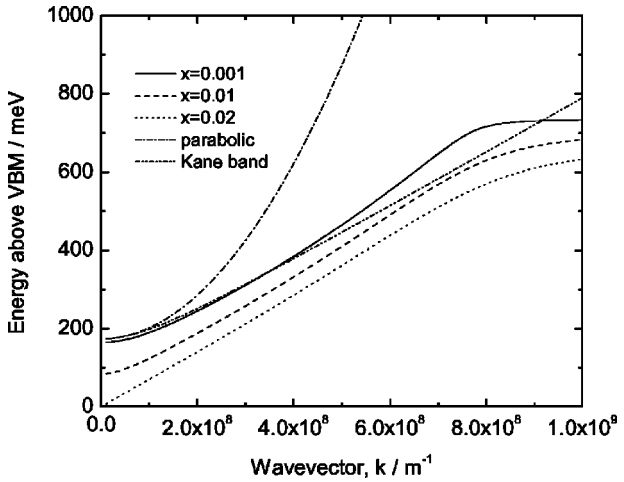

FIG. 1. The conduction band dispersion calculated for InN_xSb_{1-x} with $x = 0.001$, 0.01, and 0.02. The conduction band profile for Kane band InSb and a parabolic conduction band are also plotted for comparison.

a)Electronic mail: c.f.mcconville@warwick.ac.uk

 © 2003 American Institute of Physics
Downloaded 06 Jul 2009 to 137.205.202.8. Redistribution subject to AIP license or copyright; see http://apl.aip.org/apl/copyright.jsp

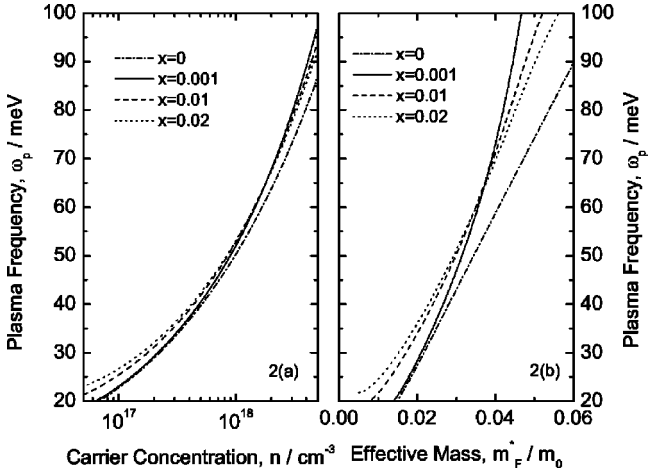

FIG. 2. The plasma frequency and the effective mass at the Fermi level calculated as a function of the carrier concentration for InN_xSb_{1-x} with $x=0.001$, 0.01, and 0.02.

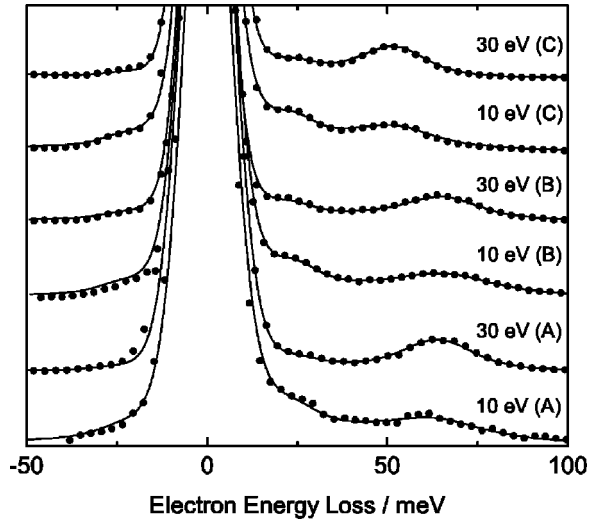

FIG. 3. Specular HREEL spectra recorded with incident electron energies of 10 and 30 eV (points) and dielectric theory simulations (solid lines) from samples A, B, and C.

to decrease as x is increased. The conduction band also undergoes a distinct flattening as it approaches the nitrogen level, resulting in enhanced effective masses at large wave vectors.

The statistics of the electrons (that is the interdependence of the plasma frequency, ω_p, the carrier concentration, n, and the effective mass at the Fermi level, m_F^*) can consequently be calculated by manipulating the E_- conduction band dispersion relation calculated for InN_xSb_{1-x}. This is achieved by first numerically integrating the product of the Fermi–Dirac distribution and the density of states in the conduction band to determine the concentration of conduction electrons. Further, the effective mass can be calculated as a function of Fermi level by exploiting its dependence on the curvature of the conduction band. Finally, the results of the first two calculations are then used to compute the plasma frequency, where the mass of the free carriers forming the plasma is that at the Fermi level. The result of these calculations with a range of x values for InN_xSb_{1-x} is shown in Fig. 2 where Fig. 2(a) shows the dependence of the plasma frequency, ω_p, on the carrier concentration, n, and Fig. 2(b) shows the variation of the effective mass at the Fermi level, m_F^*, with the plasma frequency. These plots have been calculated for $x=0.001$, 0.01, and 0.02 which corresponds to compositions with a range of band gaps from approximately that of InSb (180 meV at room temperature) to a zero band gap in $InN_{0.02}Sb_{0.98}$, respectively. The striking result of these calculations is that for this large band gap range the statistics of the electrons show a surprisingly small variation at a given plasma frequency. Consequently, if the plasma frequency of the carriers in InN_xSb_{1-x} can be determined then it is possible to define the concentration of carriers and their effective mass at the Fermi level within very small limits, even when the alloy composition is not known accurately. Alloy composition for dilute nitride alloys is normally determined from x-ray diffraction (XRD), since the incorporation of nitrogen substitutionally on group V sites reduces the lattice constant. However, this approach has not been possible for the InN_xSb_{1-x} epilayers grown so far. Nonsubstitutional nitrogen has also been incorporated, causing lattice dilation which masks the usual lattice contraction, rendering the determination of the *effective* alloy composition by XRD impossible.

Three samples of InN_xSb_{1-x}, denoted A, B, and C, were grown on InSb buffer layers by molecular beam epitaxy with nitrogen incorporation occurring by means of an electron cyclotron resonance nitrogen plasma source.[7,8] Quantification of the amount of nitrogen present in InN_xSb_{1-x} epilayers has proved to be a major difficulty.[8] However, this material represents the first fabrication of this alloy and several growth related issues still need to be resolved.[8] Crucially, the InSb buffer layer, while improving growth quality, limits the accuracy of Hall measurements because of parallel conduction, thus preventing straightforward evaluation of the electron transport properties by this method. The results of the earlier calculations indicate that, if the plasma frequency can be determined, then the electron transport properties can be evaluated within small limits.

High-resolution electron-energy-loss spectroscopy (HREELS) has been employed to probe the electronic structure in the near-surface region of these InN_xSb_{1-x} alloys. Using this technique, low-energy electrons couple to the electric fields of the surface plasmons arising from the free carriers in the conduction band resulting in electron energy loss spectra. By varying the energy of the probing electrons, the electron plasma at depths of between 100 and 1500 Å can be surveyed.[9] A series of normalized HREEL spectra, recorded from the three samples at two different incident electron energies are shown in Fig. 3, along with dielectric theory simulations. The main feature apparent in the spectra from all three samples is the conduction band plasmon peak in the range 50–65 meV. At lower probing electron energies, a surface phonon feature at ~23 meV can also be observed as a shoulder on the elastic peak. Simulation of the HREEL spectra is essential in order to extract quantitative information about the system under investigation.[9] The HREEL spectra were simulated using a two-layer model consisting of a depletion layer of thickness d and a semi-infinite bulk layer; the results of these simulations are summarized in Table I.

In addition to determining the plasma frequency of the

Downloaded 06 Jul 2009 to 137.205.202.8. Redistribution subject to AIP license or copyright; see http://apl.aip.org/apl/copyright.jsp

TABLE I. The depletion layer thickness, plasma frequency, and plasmon lifetimes extracted from the dielectric theory simulations of the HREEL spectra and the corresponding electron transport properties for samples A, B, and C.

Sample	A	B	C
d (Å)	60	70	90
ω_p (meV)	70 ± 1	68 ± 1	57 ± 1
τ (ps)	0.110	0.068	0.080
n (10^{18} cm^{-3})	2.15–2.26	2.00–2.10	1.22–1.30
m_F^*/m_0	0.039–0.040	0.038–0.039	0.033–0.034
μ (cm^2 V^{-1} s^{-1})	4800	3100	4100

electrons in the conduction band, the dielectric theory simulations also enable the plasmon lifetime, τ, to be found. However, this value of the plasmon lifetime provides only a lower limit for the bulk carrier lifetime because the measured plasmon lifetime is reduced by surface scattering and Landau damping.

Comparison of the plasma frequencies determined from the HREELS simulations with the semiconductor statistics calculated for a range of alloy compositions results in a narrow range of values for the carrier concentration and the effective mass at the Fermi level. Further, upon utilizing the usual definition of the electron mobility, a lower limit can be determined for this quantity by extracting plasmon lifetimes from the HREELS simulations and by using m_F^* obtained from the electron statistics. The results of this analysis are also presented in Table I.

The values determined for the electron effective mass at the various Fermi levels are smaller than the effective masses at equivalent Fermi levels in InSb. This result is in marked contrast to the usual increase observed in the electron effective mass in other dilute nitride alloys;[10] this is a consequence of the relatively shallow Fermi levels probed in this experiment where the conduction band is not undergoing the distinct flattening that gives rise to an increase in the electron effective mass. Hence, a distinct characteristic of dilute nitrides, the larger electron effective masses, only become apparent in InN_xSb_{1-x} when the Fermi level occupies a deeper position in energy within the conduction band where the curvature of the dispersion relation is tending towards zero. The reason for this is the extreme nonparabolicity inherent in InSb compared with the slight nonparabolicity found in GaAs. Therefore, nitrogen-induced effective mass increases are much more significant in GaN_xAs_{1-x} than in InN_xSb_{1-x} because the conduction band undergoes extreme flattening when compared with the approximately parabolic band structure in GaAs.

Although the determination of the ''active'' nitrogen content in InN_xSb_{1-x} alloys grown so far is problematic, this unknown does not significantly hinder the evaluation of the electron transport properties. This is a consequence of the small variation of the electron statistics for a wide range of InN_xSb_{1-x} compositions at a given plasma frequency. As a result, evaluating the plasma frequency and plasmon lifetime of the electrons in the conduction band of these materials enables almost complete knowledge of the electron dynamics to be ascertained. This study also demonstrates that electron effective mass enhancement only becomes apparent in InN_xSb_{1-x} when the Fermi level is high enough for the conduction band to be flattening as it approaches the nitrogen level.

The authors would like to thank T. Ashley and T. M. Burke of QinetiQ, Malvern, UK for the epitaxially grown InN_xSb_{1-x} samples and the Engineering and Physical Sciences Research Council (EPSRC) of the UK are also thanked for supporting this work under research grant GR/R93872/01.

[1] I. A. Buyanova, W. M. Chen, and B. Monemar, MRS Internet J. Nitride Semicond. Res. **2**, 2 (2001).
[2] C. Skierbiszewski, Semicond. Sci. Technol. **17**, 803 (2002).
[3] J. W. Ager III and W. Walukiewicz, Semicond. Sci. Technol. **17**, 741 (2002).
[4] E. P. O'Reilly, A. Lindsay, S. Tomic, and M. Kamal-Saadi, Semicond. Sci. Technol. **17**, 870 (2002).
[5] A. Lindsay (private communication).
[6] E. O. Kane, J. Phys. Chem. Solids **1**, 249 (1957).
[7] B. N. Murdin, A. R. Adams, P. Murzyn, C. R. Pidgeon, I. V. Bradley, J. P. R. Wells, N. Miura, T. Burke, and A. D. Johnson, Appl. Phys. Lett. **81**, 256 (2002).
[8] T. Ashley, T. M. Burke, G. J. Pryce, A. R. Adams, A. Andreev, B. N. Murdin, E. P. O'Reilly, and C. R. Pidgeon, Solid-State Electron. **47**, 387 (2003).
[9] T. D. Veal and C. F. McConville, Phys. Rev. B **64**, 085311 (2001).
[10] P. N. Hai, W. M. Chen, I. A. Buyanova, H. P. Xin, and C. W. Tu, Appl. Phys. Lett. **77**, 1843 (2000).

Downloaded 06 Jul 2009 to 137.205.202.8. Redistribution subject to AIP license or copyright; see http://apl.aip.org/apl/copyright.jsp